

# Exfoliated MoS<sub>2</sub> based Humidity Sensing

Debasree Burman<sup>1</sup>, Ravindra Kumar Jha<sup>2</sup>, Sumita Santra<sup>3\*</sup>, Prasanta Kumar Guha<sup>1\*</sup>

<sup>1</sup>Department of Electronics & Electrical Communications Engineering, IIT Kharagpur, West Bengal, 721302, India

<sup>2</sup>School of Nanoscience and Technology, IIT Kharagpur, West Bengal, 721302, India

<sup>3</sup>Department of Physics, IIT Kharagpur, West Bengal, 721302, India

\*Corresponding author, E-mail: pkguha@ece.iitkgp.ernet.in, sumita.santra@phy.iitkgp.ernet.in;

Tel: (+91) 3222-283538

Received: 31 March 2016, Revised: 01 August 2016 and Accepted: 03 September 2016

DOI: 10.5185/amp.2016/211

www.vbripress.com/amp

## Abstract

In our paper, few layered MoS<sub>2</sub> nanoflakes were exfoliated from the bulk powder in mixed solvent using a simple sonication assisted liquid exfoliation technique at room temperature. The successful exfoliation of the nanoflakes was characterized using various characterization tools like Scanning Electron Microscopy (SEM), Transmission Electron Microscopy (TEM), X-Ray Diffraction (XRD), and Atomic Force Microscopy (AFM). The humidity sensor was fabricated by drop-casting MoS<sub>2</sub> nanoflakes on Pt-based Interdigitated Electrodes (IDEs). The sensing was carried out in an in-house gas test setup interfaced with a Semiconductor Parameter Analyzer (SPA) to record the measurements. The response of the sensor was studied by passing different levels of humidity through the gas chamber. The response was found to increase with increase in humidity level and was better than few recently reported results. The maximum response was found to be ~16 times at 75% RH. Since water is an electron donor and MoS<sub>2</sub> is inherently *n*-type semiconductor, the conductivity of the MoS<sub>2</sub> sensing layer increased in presence of humidity. The large surface to volume ratio and presence of inherent defects facilitated the adsorption and desorption of a large number of H<sub>2</sub>O molecules. The response time and recovery time of the sensor was 65 seconds and 72 seconds respectively. Thus we conclude that our MoS<sub>2</sub> based humidity sensor with a maximum response of 16 times (75% RH) can act as a low power, highly sensitive and fast humidity sensor in various applications like indoor air quality monitoring, agriculture, semiconductor industry etc. Copyright © 2016 VBRI Press

**Keywords:** MoS<sub>2</sub> nanoflakes; exfoliation; humidity sensing; charge transfer; semiconductor parameter analyzer

## Introduction

The development of low-cost, high performing, portable and reliable humidity sensors is gaining importance because of their numerous applications in various control and manufacturing processes [1]. For measuring humidity, researchers have experimented with different transduction techniques like resistive, capacitive, FET, Surface Acoustic Wave (SAW), Quartz Crystal Microbalance (QCM) etc. The current focus is on resistive humidity sensors because of their capability to easily integrate with Complementary Metal Oxide Semiconductor (CMOS) technology. Recently various nanomaterials are being explored as sensing materials in humidity sensors. Graphene, a two-dimensional nanomaterial, has brought a revolution in microelectronics industry and various other application areas because of its large surface to volume ratio and unique mechanical and electrical properties [2-5]. But the lack of inherent defects does not make it a good sensing material. Its sensitivity towards humidity is quite low [6]. Molybdenum disulphide (MoS<sub>2</sub>), a two-dimensional dichalcogenide with S-Mo-S monolayers held together by weak van

der Waals force of interaction, is a relatively new nanomaterial of interest among researchers [7]. The inherent defect sites can be used as adsorption sites for the water molecules which eventually can show a change in conductivity of the sensing material. MoS<sub>2</sub> has found various applications in fuel cell, solar cell, lithium (Li) ion batteries, transistors and supercapacitors [8-15].

As per the knowledge of the authors, there have only been few reports on MoS<sub>2</sub> based humidity sensors [16-19].

In our paper, we have used a simple, room temperature, sonication based exfoliation technique to exfoliate few layered MoS<sub>2</sub> nanoflakes from its bulk powder. Various characterization tools like Scanning Electron Microscopy (SEM), Transmission Electron Microscopy (TEM), X-Ray Diffraction (XRD), and Atomic Force Microscopy (AFM) were used to characterize the nanoflakes. Next, the humidity sensor device was fabricated by drop-casting the nanoflakes on Pt electrodes. An in-house gas sensing setup was used to perform the humidity sensing tests. The response was found to increase with increase in humidity level in the chamber and it

was found to be better than few of the recently reported results [16, 17, 19]. The maximum response was found to be ~16 times at 75% RH. Since water is an electron donor [1] and MoS<sub>2</sub> is inherently an *n*-type semiconductor, [14] the conductivity of the MoS<sub>2</sub> sensing layer increases in presence of humidity. The response and recovery times were also found to be very small. Thus MoS<sub>2</sub> based sensing layer can be used to develop low power, highly sensitive and fast humidity sensor.

## Experimental

### Materials

MoS<sub>2</sub> powder (99%, Alfa Aesar) and pure ethanol (Changshu Yangyuan Chemical, China) were required for the exfoliation process. For fabricating the humidity sensors, Pt interdigitated electrodes were purchased from Synkera Technologies (Planar IDE Pt 0.25" P/N 610).

### Materials and Method

The synthesis technique that we have used in our paper was a simple sonication based exfoliation technique using mixed solvent [20]. In brief, 90mg of bulk MoS<sub>2</sub> powder was added to 45% ethanol water in a beaker. The mouth of the beaker was sealed with Parafilm and the solution was sonicated for 8 hours in a sonication bath (Oscar Ultrasonic Cleaner, Microclean 102). After sonication, centrifugation was carried out at 4500 rpm for 10 minutes to separate the supernatant from the bulk, un-exfoliated residues. The supernatant containing the nanoflakes was separately stored in vials for further characterizations and gas sensing tests.

### Material Characterizations

Various characterizations viz. SEM, AFM, TEM and XRD were performed to ensure successful exfoliation of few layered MoS<sub>2</sub> nanoflakes from the bulk powder. SUPRA 40 Field Emission Scanning Electron Microscope was used to study the surface morphology. The samples for SEM characterization were prepared by spin coating the MoS<sub>2</sub> dispersion on clean Si/SiO<sub>2</sub> substrate. Gold coating was done on the samples before the SEM was executed. The height profile and lateral dimension of the samples were obtained using Agilent Technologies AFM, Model No. 5500 in a tapping mode. The High Resolution TEM (HRTEM) images were taken by JEOL JEM-2100 HRTEM at an acceleration voltage of 200kV. The HRTEM characterization samples were prepared on a standard holey carbon covered copper grid. A Panalytical X'Pert Pro Diffractometer having a conventional X-ray tube (Cu K $\alpha$  radiation) was used to capture and analyse the diffraction patterns.

### Device fabrication and Gas Sensing Setup

For the fabrication of the humidity sensor, Pt interdigitated electrodes (IDEs) were used as the

working electrodes. MoS<sub>2</sub> nanoflakes were drop-casted on the IDEs using a micropipette. The device was probed in the gas sensing setup to study the response in presence of humidity. The schematic of the sensor device is shown in **Fig. 1(a)**.

The gas setup consisted of a stainless steel chamber where the samples were probed, a test fixture AGILENT 16442A, Semiconductor Parameter Analyzer (SPA) Agilent 4155C to record the change of humidity, gas bubblers and compressed air. There were two gas lines at the inlet of the chamber-one for the dry air and the other for humid air which was passed through a gas bubbler. The humidity values were set using a commercial humidity sensor (Dolphin Automation, Model No TH-382). The test fixture was used to interface between the sensing setup and the SPA. Two Source Measure Units (SMUs) from the SPA were used for the resistive measurements. The SMUs supplied a constant voltage and the change of current was recorded against various levels of humidity. The chamber was initially purged with dry air for 30 minutes to get a stable baseline current. **Fig. 1(b)** shows the schematic of the gas sensing setup.

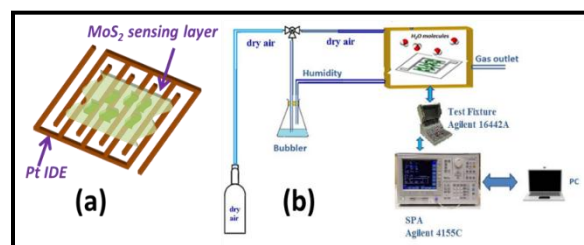


**Fig. 1.** (a) Schematic of humidity sensor device. (b) Schematic of gas test setup with sensor device probed inside the chamber.

## Results and discussion

### Characterization results

**Fig. 2 (a)** and **(b)** show the SEM images of bulk and MoS<sub>2</sub> nanoflakes respectively. As can be observed, the number of layers decreased after 8 hours of sonication.

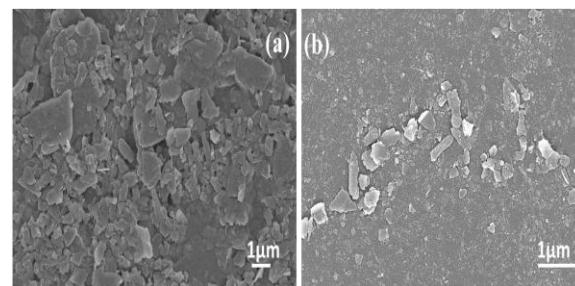


**Fig. 2.** SEM image of (a) bulk MoS<sub>2</sub> powder. (b) exfoliated MoS<sub>2</sub> nanoflakes.

The lateral dimension of the nanoflakes also reduced to ~400 nm whereas the bulk has a dimension of few micrometres. The AFM image in **Fig. 3** gives us an idea about the number of layers present in the flakes.

The height profile of a particular flake is observed to be around 16 nm implying the presence of 21-22 monolayers. The lateral dimension of the flake was nearly 500 nm.

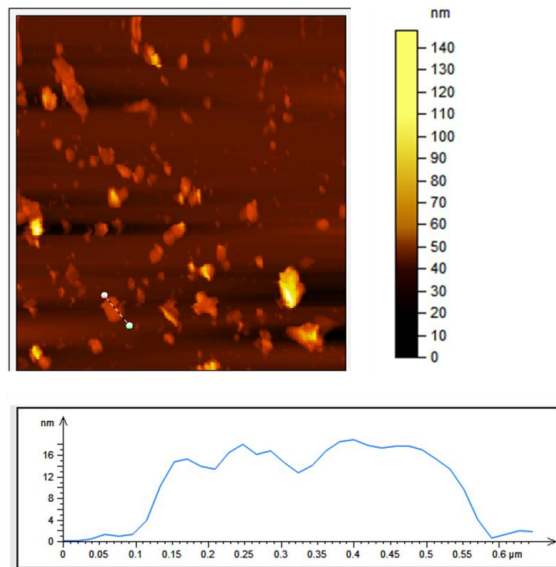


**Fig. 3.** AFM image showing the height profile and lateral dimension of the exfoliated MoS<sub>2</sub> nanoflake.

HRTEM images were helpful in providing the microstructural information of the MoS<sub>2</sub> nanoflakes. The nanoflakes in **Fig. 4(a)** show the two dimensional nature of the nanoflakes. The lattice fringes in **Fig. 4(b)** and **Fig. 4(c)** correspond to the (006) plane [ $d=0.2\text{nm}$ ] and (103) plane [ $d=0.23\text{nm}$ ] of hexagonal MoS<sub>2</sub> respectively. The SAED pattern as shown in **Fig 4(d)** reflects the crystalline structure of MoS<sub>2</sub> with a six-fold symmetry.

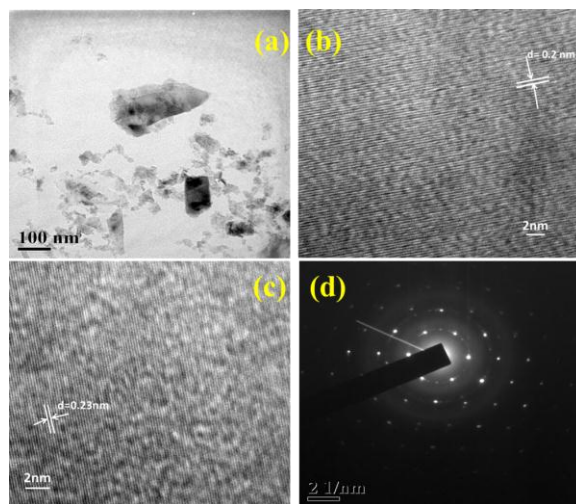


**Fig. 4.** (a) HRTEM image of exfoliated MoS<sub>2</sub> nanoflakes. (b) and (c) show fringe patterns corresponding to (006) and (103) planes respectively. (d) SAED pattern of hexagonal MoS<sub>2</sub>.

The XRD patterns of the bulk and exfoliated MoS<sub>2</sub> samples are provided in **Fig 5**. The diffraction peaks are shown in the range of  $10^0$ -  $70^0$  attributing to the standard hexagonal 2H-MoS<sub>2</sub> structure<sup>21</sup>. The lines

were indexed as per ICDD-JCPDS card no-0037-1492. The bulk shows a very strong peak at  $2\theta=14.4^0$  (002 plane) whereas the peak intensity reduces for the exfoliated sample. This implies that exfoliation has occurred across the (002) plane. Also peak broadening is observed for the exfoliated sample.

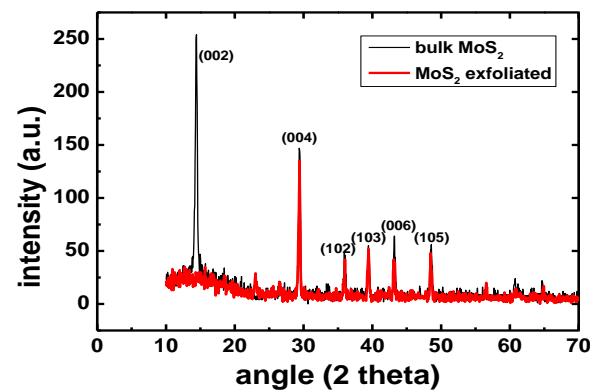


**Fig. 5** XRD patterns of bulk powder and exfoliated MoS<sub>2</sub> samples.

In order to achieve a stable baseline, the device was initially exposed to compressed air at room temperature (compressed air has relative humidity level of 25%). Four different levels of humidity (35% RH, 50% RH, 65% RH and 75% RH) were passed through the chamber each for a period of 10 minutes followed by compressed air cycles of 10 minutes each. The conductivity of the sensing material was found to vary in the presence of humidity. The response calculation was done using the following formula:

$$I_{\text{humidity}} / I_{\text{baseline}}$$

where  $I_{\text{baseline}}$  is the baseline current in presence of compressed air and  $I_{\text{humidity}}$  was the measured current in humidity. The response of the sensor for different humidity levels is shown in **Fig 6(a)**.

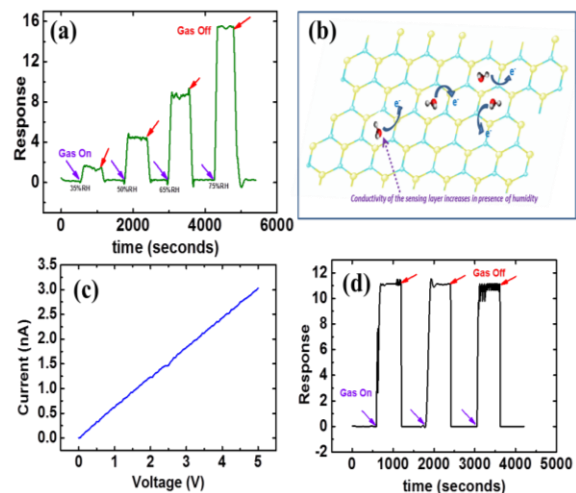


**Fig. 6.** (a) Sensing response of the sonicated sample at 4 different RH levels viz. 35%, 50%, 65% and 75% RH (b) Schematic of the sensing mechanism. (c) IV curve showing the existence of Ohmic contact. (d) Repeatability of the sensor device for three cycles at 65% RH.

It was observed that the response i.e. conductivity of the sensors increased in presence of humidity. Semiconducting MoS<sub>2</sub> is *n*-type [14] and water molecules being an electron donor enhances the conductivity of the MoS<sub>2</sub> sensing layer [1]. The charge transfer between MoS<sub>2</sub> and water molecules plays a significant role in sensing [16]. When humidity is passed through the gas chamber, the H<sub>2</sub>O molecules get physisorbed on the MoS<sub>2</sub> surfaces preferably on the top of MoS<sub>2</sub> hexagons [22]. The semiconducting MoS<sub>2</sub> sensing layer being inherently *n*-type, the conductance increases in presence of the adsorbed water molecules.

Generally, when humidity is passed, the OH<sup>-</sup> ions from the water molecules get chemisorbed at the defect sites of MoS<sub>2</sub>. Then charge transfer occurs by proton hopping [23] through the adsorbed water molecules which form a film over the chemisorbed hydroxyl ions. A schematic of the sensing mechanism is shown in Fig. 6(b).

The I-V response was measured in order to ensure proper connectivity across the contact electrodes and the probe needles. The I-V sweep in Fig. 6(c) shows proper Ohmic contact. In order to test the repeatability of the device, the device was exposed to three cycles of 65% RH each followed by a compressed air purging cycle of ten minutes each. The results in Fig. 6(d) show quite a repeatable behavior of our sensor device.

The response time was the time taken by the sample to reach 90% of the set humidity level whereas recovery time was the time taken by the sample to reach 10% of the baseline after humidity supply was closed. The response and recovery times at 65% RH were calculated to be around 65 seconds and 72 seconds respectively. The recovery is quite fast because of the intrinsic hydrophobic property of MoS<sub>2</sub> [16] that aids in the desorption of water molecules.

## Conclusion

In our work, we have tried to fabricate a resistive humidity sensor using few layered MoS<sub>2</sub> nanoflakes as the sensing material. The response of the device was tested against different levels of humidity. The response was found to increase in presence of humidity. The maximum response was found to be 16 times at a humidity level of 75% RH. The response was better than few of the previously reported results. The sensing mechanism has also been explained. The device shows a repeatable behavior and the response and recovery times are also quite low. Thus we believe that our MoS<sub>2</sub> based sensor device will be able to compete with other commercial humidity sensors in the sensor market.

## Acknowledgements

P.K. Guha acknowledges SRIC, IIT Kharagpur (ISIRD), for supporting this work partially. S. Santra acknowledges Department

of Science and Technology (DST), India, for the partial support of the work (project no. SR/S2/RJN-104/2011).

## References

1. Zhang, D.; Tong, J.; Xia, B. *Sens. Actuators, B.* **2014**, *197* (0), 66.
2. Low, T.; Avouris, P. *ACS Nano.* **2014**, *8* (2), 1086.
3. Chen, S.; Bao, P.; Xiao, L.; Wang, G. *Carbon*, **2013**, *64* (0), 158.
4. Verma, V. P.; Das, S.; Lahiri, I.; Choi, W. *Appl. Phys. Lett.* **2010**, *96* (20), -.
5. Ghosh, R.; Singh, A.; Santra, S.; Ray, S. K.; Chandra, A.; Guha, P. K. *Sens. Actuators, B.* **2014**, *205* (0), 67.
6. Ghosh, R.; Midya, A.; Santra, S.; Ray, S.; Guha, P.; Humidity Sensing by Chemically Reduced Graphene Oxide. In *Physics of Semiconductor Devices*, Jain, V. K.; Verma, A., Eds. Springer International Publishing: **2014**; Chapter 180, pp 699-701.
7. Pumera, M.; Sofer, Z.; Ambrosi, A. *J. Mater. Chem. A.* **2014**, *2* (24), 8981.
8. Hinnemann, B.; Moses, P. G.; Bonde, J.; Jørgensen, K. P.; Nielsen, J. H.; Horch, S.; Chorkendorff, I.; Nørskov, J. K. *J. Am. Chem. Soc.* **2005**, *127* (15), 5308.
9. Yue, G.; Wu, J.; Xiao, Y.; Huang, M.; Lin, J.; Lin, J.-Y. *J. Mater. Chem. A.* **2013**, *1* (4), 1495.
10. Reynolds, K. J.; Barker, J. A.; Greenham, N. C.; Friend, R. H.; Frey, G. L. *J. Appl. Phys. (Melville, NY, U. S.)*, **2002**, *92* (12), 7556.
11. Perkins, F. K.; Friedman, A. L.; Cobas, E.; Campbell, P. M.; Jernigan, G. G.; Jonker, B. T. *Nano Lett.* **2013**, *13* (2), 668.
12. Guo, J.; Chen, X.; Yi, Y.; Li, W.; Liang, C.; *RSC Adv.* **2014**, *4* (32), 16716-16720.
13. Huang, K.-J.; Zhang, J.-Z.; Shi, G.-W.; Liu, Y.-M.; *Electrochim. Acta*, **2014**, *132* (0), 397-403.
14. RadisavljevicB; RadenovicA; BrivioJ; GiacomettiV; KisA; *Nat Nano.*, **2011**, *6* (3), 147-150.
15. Hong, S. S.; Kundhikanjana, W.; Cha, J. J.; Lai, K.; Kong, D.; Meister, S.; Kelly, M. A.; Shen, Z.-X.; Cui, Y., *Nano Lett.*, **2010**, *10* (8), 3118-3122.
16. Zhang, S.-L.; Choi, H.-H.; Yue, H.-Y.; Yang, W.-C.; *Curr. Appl. Phys.*, **2014**, *14* (3), 264-268.
17. Tan, Y.; Yu, K.; Yang, T.; Zhang, Q.; Cong, W.; Yin, H.; Zhang, Z.; Chen, Y.; Zhu, Z.; *J. Mater. Chem. C.* **2014**, *2* (27), 5422-5430.
18. Donarelli, M.; Prezioso, S.; Perrozzi, F.; Bisti, F.; Nardone, M.; Giancaterini, L.; Cantalini, C.; Ottaviano, L.; *Sens. Actuators, B* **2015**, *207, Part A* (0), 602-613.
19. Chen, M.; Wi, S.; Nam, H.; Priessnitz, G.; Liang, X.; *J. Vac. Sci. Technol. (N. Y., NY, U. S.)*, **2014**, *32* (6), 06FF02.
20. Zhou, K.-G.; Mao, N.-N.; Wang, H.-X.; Peng, Y.; Zhang, H.-L.; *Angew. Chem., Int. Ed. Engl.*, **2011**, *50* (46), 10839-10842.
21. Tai, S.-Y.; Liu, C.-J.; Chou, S.-W.; Chien, F. S.-S.; Lin, J.-Y.; Lin, T.-W.; *J. Mater. Chem.*, **2012**, *22* (47), 24753-24759.
22. Yue, Q.; Shao, Z.; Chang, S.; Li, J.; *Nanoscale Res. Lett.*, **2013**, *8* (1), 1-7.
23. Yamazoe, N.; Shimizu, Y.; *Sens. Actuators*, **1986**, *10* (3-4), 379-398.